

Short Communication

Castor-Bean Extract as an Inhibitor for Low Carbon Steel Corrosion in Simulated Oilfield Produced Water

Ming Xie^{1,2*}, Peng Wang^{1,2}, Jiahao Liu^{1,2}, Ling Jian^{3*}

¹ College of Civil Engineering, Xijing University, Xi'an 710123, China

² Shaanxi Key Laboratory of Safety and Durability of Concrete Structures, Xi'an 710123, China

³ School of Economics and Management, China University of Petroleum, Qingdao, 266580, China

*E-mail: xieming_xijing@sina.com and bebetter@upc.edu.cn

Received: 4 March 2021 / Accepted: 4 June 2021 / Published: 30 June 2021

Here, a green extraction of castor-bean (GECB) as an inhibitor was used for anti-corrosion enhancement of low carbon steel plates in simulated oilfield produced water (SOPW). The analysis was performed by electrochemical impedance spectroscopy (EIS), polarization and scanning electron microscopy evaluation. The EIS analysis indicated that the charge-transfer resistance values were considerably increased as the concentration of GECB inhibitor increased in the SOPW which exhibited that the existence of GECB caused to improve the corrosion resistance of low carbon steel plate. The polarization assessment reveals that the GECB addition increased the corrosion resistant performance in low carbon steel plates noticeably with the formation of protective passive film. FESEM images of the samples indicate that the corrosion pits formed on the steel surface were reduced when GECB was added to SOPW, which is compatible with obtained electrochemical results. These results revealed that extraction of the castor-beans acted as a proper corrosion inhibitor and had a main participation in the inhibition process since it indicated 72% of inhibitor efficiency for 100 mg/L.

Keywords: Green extraction of castor-bean; Corrosion inhibitor; simulated oilfield produced water; Electrochemical evaluation

1. INTRODUCTION

Carbon steel is almost the most common building material for pipelines in the gas and oil industry [1, 2]. However, carbon steels are sensitive to corrosion in the environment, including oilfield produced water (OPW). Thus, the corrosion of the steels in OPW has become a significant issue [3].

Problems arising from OPW corrosion have caused the development of different techniques for corrosion control [4]. Using inhibitors has been recognized as the most economical and a very practical technique for combating OPW corrosion [5]. Most inhibitors are synthetic chemicals. Although their inhibitory efficiency is excellent, their high toxicity may not be ignored [6, 7].

China has a variety of oleaginous plants, including castor bean, oil palm, cotton, and soy bean, all of which have suitable chemical compounds for composition [8, 9]. Moreover, they usually present high levels of carbohydrates and proteins, oxygen-rich organic compounds and nitrogen, elements that are commonly used to inhibit corrosion [10, 11]. Furthermore, castor beans are high in protein. Sathiyathan et al. used a castor leaf ethanolic extract as an inhibitor for carbon steel in 3.5 wt% NaCl solution [12]. By electrochemical and gravimetric tests, they determined that the substrate operated as a mixed inhibitor, getting 84% efficiency for 300mgL⁻¹ extract. Abdulwahab considered the castor oil to inhibit the corrosion of Al alloys in H₃PO₄ and HCl solutions [13]. The electrochemical assessments revealed that the resistance in the 2M H₃PO₄ was more efficient, forming a passivating layer created by the fatty acid in the oil.

Although much research has been done on corrosion behavior of low carbon steel in the oilfield wastewater environment, no reports are available on the corrosion behavior of low carbon steels in SOPW. The aim of this study is to consider and assess the efficiency of a green extraction of castor-bean (GECB) for the corrosion behavior of low carbon steel in the new proposed SOPW. For this purpose, electrochemical methods such as EIS and potentiodynamic polarization were used.

2. MATERIALS AND METHODS

In order to evaluate the effect of GECB inhibitor on corrosion behavior of low carbon steel plates, electrochemical tests were performed on steel plates with a thickness of 3 mm, length of 5 cm and width of 5 cm in simulated oilfield produced water (SOPW). The composition of the used low carbon steel is shown in Table 1.

Table 1. The compositions of low carbon steel plate (wt%)

C	Mn	Cu	P	Si	Ni	S	Fe
0.09	0.48	0.15	0.012	0.04	0.05	0.02	Residual

The steel plates were cleaned with silicon carbide paper, and then washed and dipped in DI water and acetone.

Castor beans are purchased from a local Chinese market. 30 g of CBs were positioned in 400 mL of double distillation of boiling water for one hour infusion. Cotton was used for filtration, and the filtrates were packaged and frozen at -8°C. Then, the frozen filtrates were lyophilized at a temperature of -60°C, producing a powder as the final product. The physical properties of used castor bean extract have been summarized in table 2.

Table 2. Physical properties of used castor bean extract

Density (g/mL)	0.959
Viscosity (centistokes)	889.3
Thermal conductivity (W/m°C)	4.73
Specific heat (kJ/kgK)	0.089
Pour point (°C)	2.7
Flash point (°C)	145
Refractive index	1.48
Melting point (°C)	-2 to -5

The SOPW as basic test solution with a pH of 8 was prepared by deionized water and analytical grade reagents; the chemical compositions are shown in Table 3.

Table 3. Chemical composition of simulated oilfield produced water

Composition	NaCl	MgCl ₂	KCl	CaCl ₂	NaHCO ₃	Na ₂ SO ₄	Na ₂ CO ₃
Content (g/ L)	16.62	1.66	0.35	0.51	3.06	1.11	0.03

A three-electrode cell was applied during the electrochemical assessments, with low carbon steel, platinum and saturated-calomel electrodes as working, counter and reference electrodes, respectively. The EIS analysis was done at the frequency range between 100 kHz and 0.01 Hz at 10mV. The polarization characterization was performed at a scan rate of 1 mV/s. In this work, the experiments were done in 500 mL of SOPW with concentration of 0, 25, 50 and 100 mg/L GECB inhibitor which are shown as GECB0, GECB25, GECB50 and GECB100, respectively. The surface morphology of the steel specimens was conducted by a scanning electron microscope (SEM).

3. RESULTS AND DISCUSSION

The Nyquist plots of low carbon steel plates into the SOPW with different concentrations of GECB inhibitor at after immersion time of 48 h at room temperature are indicated in Figure 1. The entire semicircular loop was revealed when the sample was exposed to the SOPW without inhibitor, as shown in Fig. 1. The samples subjected to the SOPW with GECB inhibitor had an incomplete semicircle loop and a larger radius than the samples without the inhibitor, indicating that the GECB inhibitor has a significant corrosion behavior. As the inhibitor content of SOPW increased, the semicircle loop diameter increased due to the formation of a passive film or adsorption of GECB in the

anodic site of low carbon steel, which reduces iron dissolution [14]. The passive layer decreases the attack of corrosive ions on the steel surface and proficiently controls the pitting corrosion. Figure 2 indicated an equivalent circuit model used in this work. R_s presents solution resistance. C_f and R_f show the capacitance and the resistance of the passive layer, respectively [15]. R_{ct} and C_{dl} present the charge-transfer resistance and double-layer capacitance of the low carbon steel surface, respectively [16]. The obtained results are exhibited in Table 3.

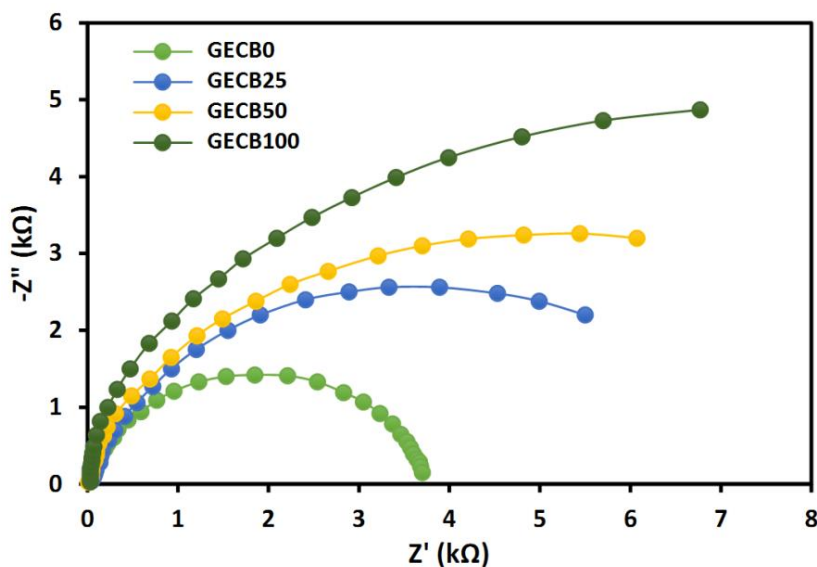


Figure 1. EIS diagrams of low carbon steel plates into the SOPW with different concentration of GECB inhibitor at after immersion time of 48 h.

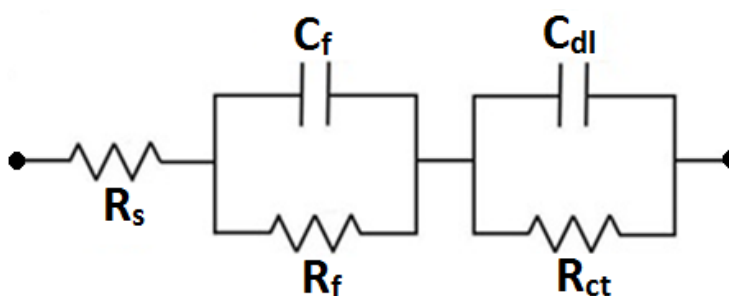


Figure 2. A circuit model

The best fitting results are shown in Table 4. As indicated, the R_{ct} values were considerably increased from 3.6 kΩ to 12.8 kΩ, as the concentration of GECB inhibitor increased in the simulated oilfield produced water which exhibited that the existence of GECB caused to improve the corrosion resistance of low carbon steel plate.

Table 4. The best fitting results obtained from equivalent circuit for low carbon steels into the simulated oilfield produced water with different concentration of GECB inhibitor after immersion time of 48 h

Inhibitor	R_s (Ω)	R_f ($k\Omega$)	C_f (μFcm^{-2})	R_{ct} ($k\Omega$)	C_{dl} (μFcm^{-2})
GECB0	28.4	2.2	19.4	3.6	29.6
GECB25	27.8	5.4	12.6	6.9	21.3
GECB50	23.6	7.1	7.8	9.7	14.8
GECB100	25.7	9.8	4.5	12.8	10.5

Inhibitor efficiency (μ_i) was measured by the following equation:

$$\mu_i (\%) = 100 \times (R_{ct} - R_{ct}^*) / R_{ct} \quad (1)$$

where R_{ct} and R_{ct}^* are the charge-transfer resistance with and without inhibitor.

Table 5 indicates the μ_i comparison of various inhibitors as mentioned in literature. As shown, the μ_i of GECB inhibitor in this study was comparable with other inhibitors gained from literature.

Figure 3 indicates the Bode plots of low carbon steel plates immersed in simulated oilfield produced water with different concentration of GECB inhibitor after immersion time of 48 h. As revealed, when inhibitor volumes were increased from 0 to 100 mg/L, the impedance values enriched 8 times, which indicates that the high amount of GECB inhibitor strangely controls the corrosion behavior of the low carbon steel in the SOPW. It can be associated with the whole cover of the active surface of low carbon steel plate by GECB inhibitor [17].

Table 5. The μ_i comparison of various inhibitors as mentioned in literature

Inhibitors	Environment	μ_i (%)	Ref.
Aloe polysaccharide	Simulated acidic oilfield water	84	[18]
Cymbopogon citratus	Produced oilfield water	47	[19]
Gemini surfactants	Oilfield produced water	68	[20]
Thiadiazole derivatives	CO ₂ -saturated oilfield produced water	98	[21]
Eucalyptus Globulus	Alkaline chloride solution	87	[22]
GECB	Simulated oilfield produced water	72.0	This work

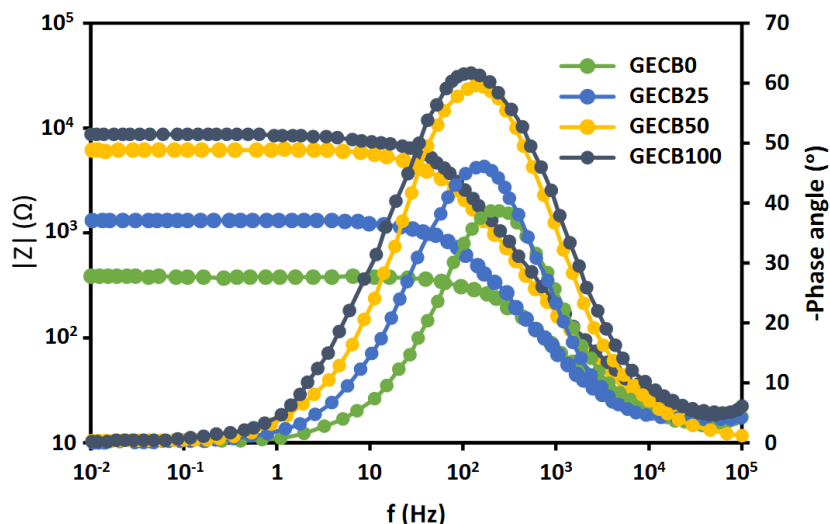


Figure 3. Bode plots of low carbon steel plates immersed in simulated oilfield produced water with different concentration of GECB inhibitor after immersion time of 48 h

Moreover, it can be correlated to the creation of passive film on steel surface by inhibitor adsorption. This layer has an important effect in preventing corrosion ions from reaching the surface of the steel. The specimens immersed in the SOPW without GECB inhibitors were more sensitive to corrosion due to corrosive ions attack on the steel surface. Thus, a decrease in impedance values was observed in SOPW containing GECB inhibitor. As indicated in figure 3, the maximum phase angle for steel plates in simulated oilfield produced water containing GECB inhibitors at a lower-frequency were shifted to higher angles because of the formation of protective passive film [23]. The phase angles were shifted from -61° to -63° in SOPW with 50 and 100 mg/L GECB, showing the passive film was homogenous and uniform.

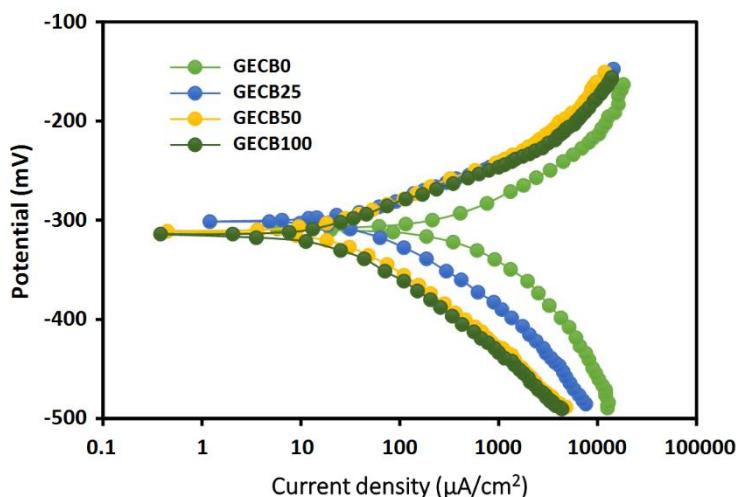


Figure 4. The polarization plots of low carbon steel in SOPW without and with GECB at 25, 50, and 100 mg/L

Figure 4 reveals the polarization plots of low carbon steel in SOPW without and with GECB at 25, 50, and 100 mg/L. Table 5 shows the kinetic parameters derived from the Tafel extrapolation technique. Figure 4 shows that the existence of GECB regardless of its content causes the reduction of the current density of both branches.

Inhibition efficiency (μ_i) of GECB in the SOPW is also indicated in Table 6. The μ_i is calculated as:

$$\mu_i (\%) = 100 \times (i_{\text{corr}} - i_{\text{corr}}^*) / i_{\text{corr}} \tag{2}$$

where i_{corr}^* and i_{corr} present the value of corrosion current density without and with GECB inhibitors, respectively. The increase in GECB content resulted in a reduction of current density, once compared to blank, enhancing the values of inhibition efficiency and obtaining a maximum μ_i value of 90.3% at 100 mg/L, approving the above discussion about the formation of protective layer. After 50 mg/L of GECB, the μ_i value increases very slight for long exposure time.

Table 6. The kinetic parameters derived from the Tafel extrapolation technique

Inhibitor	Corrosion current density ($\mu\text{A}/\text{cm}^2$)	Corrosion potential (V)	$-\beta_c$ (mVdec^{-1})	β_a (mVdec^{-1})	μ_i (%)
GECB0	819	-316	132	68	-
GECB25	216	-304	117	59	73.6
GECB50	88	-321	121	54	89.2
GECB100	79	-424	123	57	90.3

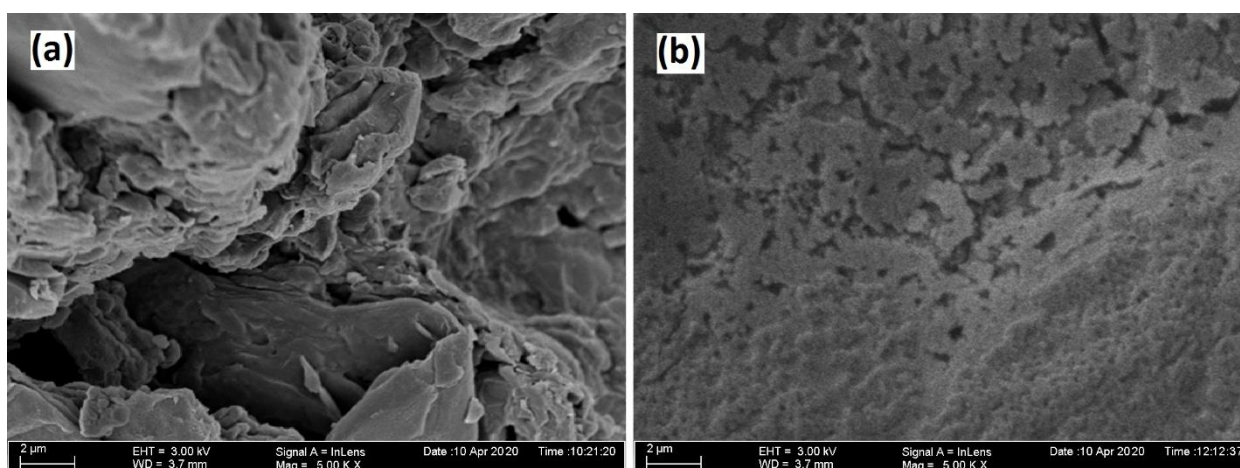


Figure 5. SEM images of low carbon steel plates into the SOPW (a) without (b) with GECB inhibitor after exposure time of 48 h

Furthermore, it is found that by increasing GECB content, the E_{corr} was shifted toward more positive value. The maximum shift of E_{corr} was obtained for 100 mg/L GECB. Generally, Tafel slopes

for cathodic and anodic reactions change very slight by adding the inhibitors, which reveals the small difference of the β_c and β_a constants. Given that the GECB addition indicated a reduction of β_a , the GECB acts as an inhibitor in the organic compounds in which the screening effect was added to activation effects.

Figure 5 shows SEM images of low carbon steel plates in the SOPW with varying concentrations of GECB inhibitor after a 48-hour exposure time at room temperature. The surface of the low carbon steel plate exposed to the SOPW with 100 mg/L of GECB inhibitor exhibited low corrosion products and thin pits, revealing a small pitting corrosion shaped on the steel plate surface, which is according to the results attained from electrochemical analysis.

4. CONCLUSION

In this work, GECB was used as an inhibitor for anti-corrosion enhancement of low carbon steel plates in the SOPW. The analysis was performed by EIS, polarization and SEM evaluations. The EIS analysis indicated that the charge-transfer resistance values were considerably increased as the concentration of GECB inhibitor increased in the SOPW which exhibited that the existence of GECB caused to improve the corrosion resistance of low carbon steel plate. The polarization assessment reveals that the GECB addition increased the corrosion resistant performance in low carbon steel plates noticeably with the formation of protective passive film. SEM images of a low carbon steel plate exposed to the SOPW with 100 mg/L of GECB inhibitor exhibited low corrosion products and thin pits, revealing a small pitting corrosion shaped on the steel plate surface, which is according to the results attained from electrochemical analysis. These results revealed that extraction of the castor-beans acted as a proper corrosion inhibitor and had a main participation in the inhibition process since it indicated 72% of inhibitor efficiency for 100 mg/L.

ACKNOWLEDGEMENT

This work was sponsored in part by High-level Talents Special Foundation of Xijing University (XJ17B04)

References

1. I.B. Obot, I.B. Onyeachu and S.A. Umoren, *Corrosion Science*, 159 (2019) 108140.
2. S. Kakooei, H.M. Akil, A. Dolati and J. Rouhi, *Construction and Building Materials*, 35 (2012) 564.
3. L. Quej-Ake, A. Contreras and J. Aburto, *Anti-Corrosion Methods and Materials*, 15 (2018) 15.
4. S. Lahme, J. Mand, J. Longwell, R. Smith and D. Enning, *Applied and Environmental Microbiology*, 87 (2021) 124.
5. B. Hou, Q. Zhang, Y. Li, G. Zhu, H. Liu and G. Zhang, *Corrosion Science*, 164 (2020) 108334.
6. G. Bahlakeh, B. Ramezanzadeh, A. Dehghani and M. Ramezanzadeh, *Journal of Molecular Liquids*, 283 (2019) 174.
7. J. Rouhi, S. Kakooei, M.C. Ismail, R. Karimzadeh and M.R. Mahmood, *International Journal of Electrochemical Science*, 12 (2017) 9933.

8. F. Takahashi and E. Ortega, *Energy Policy*, 38 (2010) 2446.
9. A. Khanra, M. Srivastava, M.P. Rai and R. Prakash, *ACS omega*, 3 (2018) 12369.
10. C. Charnier, E. Latrille, J.-M. Roger, J. Miroux and J.-P. Steyer, *Chemical Engineering & Technology*, 41 (2018) 727.
11. A. Santos, I. Aquino, F. Cotting, I. Aoki, H. De Melo and V. Capelossi, *Metals and Materials International*, 17 (2020) 1.
12. R. Sathiyathan, S. Maruthamuthu and M.M. Selvanayagam, *Indian J. Chem. Technol*, 12 356.
13. M. Abdulwahab, A. Popoola and O. Fayomi, *International Journal of Electrochemical Science*, 7 (2012) 11706.
14. A. Fouda, G. Elewady, K. Shalabi and H.A. El-Aziz, *RSC Advances*, 5 (2015) 36957.
15. K.M. Emran and H. AL-Refai, *International Journal of Electrochemical Science*, 12 (2017) 6404.
16. N. Naderi, M. Hashim, K. Saron and J. Rouhi, *Semiconductor Science and Technology*, 28 (2013) 025011.
17. Y. Cao, S. Dong, D. Zheng, J. Wang, X. Zhang, R. Du, G. Song and C. Lin, *Corrosion Science*, 126 (2017) 166.
18. W. Zhang, Y. Ma, L. Chen, L.-J. Wang, Y.-C. Wu and H.-J. Li, *Journal of Molecular Liquids*, 307 (2020) 112950.
19. M. Deyab, M. Osman, A. Elkholy and F.E.-T. Heakal, *RSC advances*, 7 (2017) 45241.
20. M. Migahed, M. El-Rabiei, H. Nady and E. Zaki, *Journal of Molecular Structure*, 1159 (2018) 10.
21. Q. Zhang, B. Hou and G. Zhang, *Journal of colloid and interface science*, 572 (2020) 91.
22. N. Etteyeb and X. Nóvoa, *Corrosion Science*, 112 (2016) 471.
23. H.-S. Ryu, J.K. Singh, H.-S. Lee, M.A. Ismail and W.-J. Park, *Construction and Building Materials*, 133 (2017) 387.